18

Finite-time Scaling and its Applications to Continuous Phase Transitions

Fan Zhong
State Key Laboratory of Optoelectronic Materials and Technologies
School of Physics and Engineering, Sun Yat-sen University, Guangzhou 510275
People's Republic of China

1. Introduction

Monte Carlo methods of numerical simulations play an important role in studying phase transitions in general and critical phenomena in particular in statistical physics (Amit & Martin-Mayor, 2005; Binder & Heermann, 1988; Landau & Binder, 2005; Newman & Barkema, 1999). A hallmark of the critical phenomena that a system exhibit in the vicinity of a second-order phase transition, or in the modern classification, continuous phase transition (Fisher, 1967) is its diverging correlation length (Amit & Martin-Mayor, 2005; Cardy, 1996; Ma, 1976; Stanley, 1971). This length scale renders at first sight numerical simulations useless because they are inevitably carried out on systems of finite sizes that are thus smaller than the correlation length and thus cannot probe the bulk behavior of the system under considered. Moreover, real phase transitions occur only in the thermodynamic limit.

Yet, the idea of finite-size scaling has turned this nuisance into a blessing and the method based on it has become a routine to extract critical properties from numerical simulations of finite systems (Amit & Martin-Mayor, 2005; Cardy, 1988; Fisher & Ferdinand, 1967; Fisher & Barber, 1972; Gasparini et al., 2008; Landau & Binder, 2005; Privman, 1990). Under the assumption that upon a renormalization-group transformation of a length rescaling of factor b, the coupling constants of a finite system transform in the same way as in the thermodynamics limit (Brézin, 1982; Brézin & Zinn-Justin, 1985), the singular part of the free energy of the system then transforms as

$$F(\tau, H, L^{-1}) = b^{-d} F(\tau b^{1/\nu}, H b^{\beta\delta/\nu}, L^{-1} b), \tag{1}$$

where δ, β, and ν are critical exponents, L is a characteristic length scale of the system, d the spatial dimensionality, H the external magnetic field (we shall use the terminology of magnetism throughout), and the reduced temperature $\tau = T - T_c$ with T_c being the critical temperature. As a result, one arrives at the finite-size scaling ansatz for the free energy

$$F(\tau, H, L^{-1}) = L^{-d} f(\tau L^{1/\nu}, H L^{\beta\delta/\nu}), \tag{2}$$

where f is a scaling function. We have neglected possible dimensional factors for conciseness hereafter. Appropriate differentiations of Equation (2) then give rise to corresponding scaling forms for the magnetization M, the susceptibility χ, and the specific heat C as

$$M(\tau, L) = L^{-\beta/\nu} f_1(\tau L^{1/\nu}), \tag{3a}$$
$$\chi(\tau, L) = L^{\gamma/\nu} f_2(\tau L^{1/\nu}), \tag{3b}$$
$$C(\tau, L) = L^{\alpha/\nu} f_3(\tau L^{1/\nu}) \tag{3c}$$

using the scaling laws or relations

$$\alpha = 2 - d\nu, \tag{4a}$$
$$\alpha + 2\beta + \gamma = 2, \tag{4b}$$
$$\beta\delta = \beta + \gamma, \tag{4c}$$

where α and γ are critical exponents and the fs including those that will appear later are all scaling functions. In terms of the infinite system correlation length ξ_∞ that diverges at T_c as

$$\xi_\infty \propto |\tau|^{-\nu}, \tag{5}$$

the argument of fs in Equations (3) is proportional to L/ξ_∞ that governs the finite-size behavior; for small L/ξ_∞, finite-size scaling appears in which L is a relevant length scale, while large L/ξ_∞ is the thermodynamic limit in which equilibrium behavior shows and L is irrelevant. Note that all the critical exponents assume their infinite-lattices values due to the aforemention assumption (Brézin, 1982; Brézin & Zinn-Justin, 1985). Consequently, measuring the observables for a series of L can then determine the corresponding exponent ratios and finally the critical exponents themselves, the pitch of the critical properties, from the pure power laws emerged exactly at T_c or $\tau = 0$ at which fs are assumed to be analytic. In fact, for too small systems sizes and temperatures too far away from T_c, corrections to scaling (Wegner, 1972) have to be taken into account. Nevertheless, delicate methods have been developed for extracting critical exponents as well as T_c (Amit & Martin-Mayor, 2005; Landau & Binder, 2005).

A sequence of Monte Carlo updates may be interpreted as a discrete Markov process (Glauber, 1963; Landau & Binder, 2005; Müler-Krumbhaar & Binder, 1973). Consequently, Monte Carlo simulations can also be applied to study time-dependent dynamic behavior, though usually studied is stochastic relaxational dynamics instead of 'true dynamics' in which the dynamics is determined by the equations of motion derived from a Hamiltonian. Yet, the stochastic dynamics for the kinetic Ising model with local spin dynamics as realized in the single-site Metropolis algorithm (Metropolis et al., 1953), for instance, is believed to fall into the same universality class as that governed by the time-dependent Ginzburg-Landau equation (Hohenberg & Halperin, 1977). Dynamic critical phenomena (Cardy, 1996; Ferrell et al., 1967; Folk & Moser, 2006; Halperin & Hohenberg, 1967; Hohenberg & Halperin, 1977; Ma, 1976) are also companying with a divergent correlation time t_{eq} which diverges with the correlation length ξ_∞ as

$$t_{eq} \propto \xi_\infty^z \tag{6}$$

with a new dynamical critical exponent z dynamic finite-size scaling (Suzuki, 1977) can be obtained by formally incorporating the time argument t in Equation (1), giving rise to

$$M(\tau, H, t, L^{-1}) = b^{-\beta/\nu} M(\tau b^{1/\nu}, H b^{\beta\delta/\nu}, t b^{-z}, L^{-1} b) \tag{7}$$

after a derivative with H. As a result, the finite-size scaling form of the order parameter, Equation (3a), say, now becomes

$$M(\tau, t, L) = L^{-\beta/\nu} f_{1t}(\tau L^{1/\nu}, tL^{-z}), \tag{8}$$

which implies a dynamic finite-size scaling form for the correlation time

$$t_L = L^z f_{2t}(\tau L^{1/\nu}). \tag{9}$$

Therefore, at the criticality,

$$t_L \propto L^z \tag{10}$$

in the asymptotic region of large time, large size, and small τ. This is again a standard method to estimate z, though when the asymptotic region is reached is not easy to determine (Landau & Binder, 2005; Wansleben & Landau, 1991).

However, actual simulations can only be performed inevitably in a limited time for large system sizes. So, one encounters a situation that is similar to the static case: In order to have good estimates of z, one needs to wait for a long time that is longer than t_{eq} to enter the asymptotic region similar to the static case in which one needs a large system size that is bigger than ξ. In fact, even in the static case, one also needs to wait a similar long time to the dynamic case in order for the system to equilibrate. This is in fact the issue of critical slowing down. Nevertheless, finite-size scaling has efficiently helped the static case to overcome the limited-size problem. It is then quite surprised that a finite-*time* scaling was elusive for nearly forty years except for several not-well-noticed work on disordered systems (Hukushima & Nemeto, 1995; Shima & Nakayama, 1998; 1999; Shinomoto & Kabashima, 1991). Recently, we realized that the linearly driving method we had been applying to study both first-order (Zhang & Zhong, 1996; Zhong, 2002; Zhong & Chen, 2005; Zhong et al., 1994; 1995; 1998; Zhong & Zhang, 1995a;b; 1997) and continuous phase transitions (Fan & Zhong, 2007; 2009; Zhong, 2006; Zhong & Xu, 2005) just offered a realization of such a scaling (Gong et al., 2010; Huang et al., 2010). The method provides an external effective time scale that is inversely proportional to the rate R of the driving by which either an external field or the temperature that varies linearly with time was applied to a system near its criticality. Because of this finite time scale, the system evolves according to the driving rather than by itself, which takes a long time near its criticality. As a consequence, both static and dynamic scaling behavior can be probed effectively without suffering from critical slowing down. In addition, this time scale is readily manipulable not only in simulations but also in experiments (Zhang & Zhong, 1996) and thus serves as the temporal analogue of the finite size scale, though the latter may not be so obtainable experimentally (Gasparini et al., 2008). We shall review the theory and applications of the finite-time scaling in this chapter. However, before entering into the details, we would like to make some remarks.

First, for the usual Monte Carlo simulations of phase transitions such as those on the Ising model with the usual Metropolis algorithm (Metropolis et al., 1953), a direct analogue of the finite-size scaling by measuring observables at a series of time may not work because the system needs sufficiently long time to sample its configuration space in order for the observables to be measured correctly.

Second, there exist scalings with the time or its Fourier transform frequency. However, these are not the kinds of finite-time scaling in the spirit of the finite-size scaling. The central distinction is that in finite-time scaling there is a driving that imposes on the system a finite time scale that restricts its natural evolution and thus its scaling and that is controllable in close analogue to the external length scale in finite-size scaling.

For example, in the short-time critical dynamics (Zheng, 1998), there is a new independent initial slip exponent θ associated with a small initial magnetization m_0 (Janssen et al., 1989). The dynamic transformation law for M in the absence of H is (Li et al., 1995; Zheng, 1998)

$$M(\tau, t, m_0, L) = b^{-\beta/\nu} M(\tau b^{1/\nu}, tb^{-z}, b^{x_0} m_0, L^{-1} b), \tag{11}$$

or

$$M(\tau, t, m_0, L) = t^{-\beta/\nu z} f_{3t}(\tau t^{1/\nu z}, m_0 t^{x_0/z}, L^{-1} t^{1/z}) \tag{12}$$

by setting $b = t^{1/z}$, where $x_0 = \theta + \beta/\nu$, because for a sufficiently large lattice and small m_0 at $\tau = 0$, $M \propto t^{\theta}$ in the initial stage from Equation (12). In addition, one may make a temporal Fourier transformation to the dynamics. A transformation law in terms of the frequency ω instead of t similar to Equation (7) can be written, leading then to

$$M(\tau, \omega, L) = \omega^{\beta/\nu z} f_{4t}(\tau \omega^{-1/\nu z}, L^{-1} \omega^{-1/z}). \tag{13}$$

One may regard Equations (12) and (13) as examples of finite-time scaling. However, t and its Fourier transform ω are natural evolution time of the system and cannot be varied in contrast to L in Equation (8) and R in Equations (34) and (47) below.

In the following, we shall first review briefly the theory of finite-time scaling (Section 2), then summarize the current methods to extract critical properties using finite-time scaling (Section 3), followed by a summary of the results obtained with them in continuous transitions of pure and disordered systems (Section 4). Finally, discussions on the merits and shortcomings of the methods and future studies as well as conclusions are presented in Section 5.

2. Theory of finite-time scaling

In this section, we shall first briefly review in Section 2.1 the renormalization-group theory of finite-time scaling both for a field driving (Section 2.1.1) and for a temperature driving (Section 2.1.2) to justify the scaling (Gong et al., 2010; Zhong, 2006). Then, we shall study crossovers in Section 2.2 and corrections to scaling in Section 2.3 and discuss the combined effects of both finite time and finite size by taking into account the latter in Section 2.4.

2.1 Renormalization-group theory of finite-time scaling

Consider the model with the following Ginzburg-Landau functional of a φ^4 theory in an external field H,

$$F[\varphi] = \int d\mathbf{r} \left\{ \frac{1}{2}\tau\varphi^2 + \frac{1}{4!}g\varphi^4 + \frac{1}{2}(\nabla\varphi)^2 - H\varphi \right\}, \tag{14}$$

where g is a coupling constant and τ is proportional to the temperature distance from the mean-field T_c. Its dynamics is governed by the Langevin equation for the scalar non-conserved order parameter φ,

$$\frac{\partial\varphi}{\partial t} = -\lambda \frac{\delta F[\varphi]}{\delta\varphi} + \xi \tag{15}$$

with a Gaussian white noise ξ satisfying

$$\langle \xi(\mathbf{r},t)\rangle = 0, \qquad \langle \xi(\mathbf{r},t)\xi(\mathbf{r}',t')\rangle = 2\lambda\delta(\mathbf{r}-\mathbf{r}')\delta(t-t'), \tag{16}$$

where λ is a kinetic coefficient. This is the Model A (Hohenberg & Halperin, 1977), which falls in the same universality class as the kinetic Ising model with local spin dynamics. We shall consider two driven non-equilibrium situations in which one starts with a sufficiently ordered state and increases linearly either the external field $H = Rt$ or the temperature $\tau = Rt$ with a small rate constant R across the critical point. As the critical point lies at $\tau = 0$ and $H = 0$, our choice of initial conditions means t is in fact $t - t_c$ with t_c the time at the critical point. For simplicity, however, we shall still use t below as the shift of initial point makes no difference in the linear driving, which makes in fact this driving superior to others including the usual sinusoidal driving (Gong et al., 2010).
In order to use systematic field-theoretic methods, we recast the dynamics into an equivalent field theory with a dynamic functional (Janssen, 1992),

$$I[\varphi,\tilde{\varphi}] = \int d\mathbf{r}dt\left\{\tilde{\varphi}\left[\dot{\varphi}+\lambda(\tau-\nabla^2)\varphi+\frac{1}{3!}\lambda g\varphi^3-\lambda H\right]-\lambda\tilde{\varphi}^2\right\} \tag{17}$$

by introducing an auxiliary response field $\tilde{\varphi}$ (Martin et al., 1973). Expectation values can then be obtained by taking appropriate derivatives of the generating functional

$$W[h,\tilde{h}] = \ln\int D(\varphi,\tilde{\varphi})\exp[-I[\varphi,\tilde{\varphi}] + \int d\mathbf{r}dt(h\varphi+\tilde{h}\tilde{\varphi})] \tag{18}$$

with respect to the external sources h and $\tilde{h}$ that conjugate respectively to φ and $\tilde{\varphi}$.
Accordingly to the field theoretical formulation of the renormalization-group theory, the critical exponents are associated with the renormalization factors Zs that cure the divergences in the theory (Amit & Martin-Mayor, 2005; Zinn-Justin, 1996). One notices that since the variation of T and H is spatially uniform and depends linearly on time with a small R, no new divergence except the extrinsic one at $t \to \infty$ or $\omega \to 0$ in frequency domain is generated. As a result, no new Z besides the usual φ^4–theory ones has to be introduced, except the possible initial slip (Janssen et al., 1989) which does not contribute however because the transition is independent of the initial condition when we start with a driving sufficiently far away from the critical point. To deal with the time-dependent external probes, we perform the renormalization at the critical point at which τ and H vanish, and then make an expansion about the critical theory (Amit & Martin-Mayor, 2005; Weinberg, 1973; Zinn-Justin, 1996) by taking as insertions the deviations arising from the driving away from that point. In this way, the time dependent external probes can be naturally accounted for. Moreover, the renormalization at the critical point enables us to make direct contact with the original situation to which no time-dependent field is applied, and thus to solve analytically the problem almost without any additional labor. We shall treat the cases of varying external field and varying temperature separately in the following.

2.1.1 Theory of field driving

In this case, H is varying with t linearly and τ is a small constant. The theory can be rendered finite for $d \leq 4$ by introducing the following Z factors (Amit & Martin-Mayor, 2005; Janssen, 1992; Zinn-Justin, 1996)

$$\begin{aligned} &\varphi \to \varphi_0 = Z_\varphi^{1/2}\varphi, \qquad \tilde{\varphi} \to \tilde{\varphi}_0 = Z_{\tilde{\varphi}}^{1/2}\tilde{\varphi}, \qquad g \to g_0 = N_d \mu^\epsilon Z_\varphi^{-2} Z_u u, \\ &\lambda \to \lambda_0 = (Z_\varphi / Z_{\tilde{\varphi}})^{1/2} Z_\lambda \lambda, \qquad \tau \to \tau_0 = Z_\varphi^{-1} Z_{\varphi^2}\tau + \tau_c, \qquad H \to H_0 = Z_\varphi^{-1/2} H, \end{aligned} \tag{19}$$

where $\epsilon = 4 - d$, $N_d = 2/[(4\pi)^{d/2}\Gamma(d/2)]$ with Γ being the Euler Gamma function, μ is an arbitrary momentum scale, and τ_c the fluctuation shift of the critical point, which can be neglected as dimension regulations ('t Hooft & Veltman, 1972) are employed. However, we shall henceforth still use τ to denote $\tau - \tau_c$ that is proportional to $T - T_c$. Consequently, the critical point at $\tau = 0$ and $H = 0$ can be chosen to correspond to $t = 0$ by a proper time translation. In Equation (19), the subscripts 0 indicate unrenormalized bare variables. By exploiting the fact that the bare quantities are independent of μ and expanding the averaged order parameter in a Taylor's series in τ and H at every definite time instant, namely

$$M(\tau, H) = \langle \varphi(\tau, H) \rangle = G_{10,0}(\tau, H) = \sum_{N,N'=1}^{\infty} \frac{1}{N!N'!} \lambda^{N+N'} \tau^{N'} H^N G_{1N,N'}(0,0), \tag{20}$$

the Green function $G_{1N,N'}$ is defined as

$$G_{1N,N'} = \frac{\delta^{1+N+N'} W[h, \tilde{h}, \tau]}{\delta h \delta \tilde{h}^N \delta \tau^{N'}} \tag{21}$$

the renormalization-group equation is thus,

$$\left(\mu\partial_\mu + \varsigma\lambda\partial_\lambda + \beta\partial_u + \gamma_{\varphi^2}\tau\partial_\tau + \frac{1}{2}\gamma H \partial_H + \frac{1}{2}\gamma \right) M = 0, \tag{22}$$

with the Wilson's functions being defined as derivatives at fixed bare parameters,

$$\varsigma(u) = \mu\partial_\mu \ln \lambda, \qquad \gamma(u) = \mu\partial_\mu \ln Z_\varphi, \qquad \gamma_{\varphi^2}(u) = \mu\partial_\mu \ln \tau, \qquad \beta(u) = \mu\partial_\mu u, \tag{23}$$

where ∂_i indicates the partial derivative with respect to i. No new Wilson's function due to the driving has to be introduced.

At the fixed point

$$u = u^*, \qquad \beta(u^*) = 0, \tag{24}$$

the solution of (22) is

$$M(\lambda, \tau, H, u, \mu) = \rho^{\gamma^*/2} M(\lambda\rho^{\varsigma^*}, \tau\rho^{\gamma^*_{\varphi^2}}, H\rho^{\gamma^*/2}, u^*, \mu\rho), \tag{25}$$

where ρ is a running (momentum) variable and starred quantities denote the corresponding values at the fixed point. On the other hand, from the naïve dimensions of various variables

$$\begin{aligned} &|\mathbf{r}| \propto \mu^{-1}, \qquad \tau \propto \mu^2, \qquad u \propto \mu^0, \qquad \lambda t \propto \mu^{-2}, \\ &\varphi \propto \mu^{(d-2)/2}, \qquad H \propto \mu^{(d+2)/2}, \qquad \tilde{\varphi} \propto \mu^{(d+2)/2}, \end{aligned} \tag{26}$$

one obtains a homogeneous form

$$M(\lambda, \tau, H, u, \mu) = \rho^{(d-2)/2} M(\lambda t \rho^2, \tau\rho^{-2}, H\rho^{-(d+2)/2}, u, \mu/\rho). \tag{27}$$

Applying (27) to the left-hand size of (25) leads to

$$M(t,\tau,H) = \rho^{\beta/\nu} M(t\rho^{z}, \tau\rho^{-1/\nu}, H\rho^{-\beta\delta/\nu}), \tag{28}$$

or in terms of the length variable b,

$$M(t,\tau,H) = b^{-\beta/\nu} M(tb^{-z}, \tau b^{1/\nu}, Hb^{\beta\delta/\nu}), \tag{29}$$

with the critical exponents given by

$$\eta = \gamma^{*}, \qquad \nu^{-1} = 2 - \gamma^{*}_{\varphi^2}, \qquad z = 2 + \varsigma^{*}, \tag{30a}$$

$$\beta/\nu = (d - 2 + \eta)/2, \qquad \delta = (d + 2 - \eta)/(d - 2 + \eta), \tag{30b}$$

where we have chosen λ as the time unit and used the same symbol to denote functions of different numbers with arguments.

As we perform the renormalization at the critical point and utilize the scheme of dimension regulations and minimal subtractions with ε expansion ('t Hooft & Veltman, 1972), a scheme in which dynamics decouples from statics (De Dominicis & Peliti, 1978), all the Z factors can be chosen to be identical to the usual φ^4 model. As a result, all the static critical exponents and the dynamic critical exponent z determined from (30) are identical to those of the usual scalar Model A in the absence of the time-dependent field (Zhong, 2006; Zinn-Justin, 1996). Consequently, Equation (29) is just Equation (7) in the thermodynamic limit $L^{-1} = 0$.

Now the linearly varying field $H = Rt$ can be complemented to Equation (29) (Zhong, 2006). (29) implies H and t transform as

$$H' = Hb^{\beta\delta/\nu}, \qquad t' = tb^{-z}, \tag{31a}$$

respectively, where the primes indicate variables after rescaling. In the vicinity of T_c, R should also scale upon renormalization. Suppose it transforms as

$$R' = Rb^{r_H}, \tag{31b}$$

since $H' = R't'$, one then obtains from Equation (31) a scaling law

$$r_H = z + \beta\delta/\nu, \tag{32}$$

which may be regarded as a definition of r_H that reflects the rescaling of R with that of H and t since $R = H/t$. Replacing t with R and setting $b = R^{-1/r_H}$ in Equation (29), one finds

$$M(t,\tau,R) = R^{\beta/\nu r_H} m_{1H}(tR^{z/r_H}, \tau R^{-1/\nu r_H}), \tag{33}$$

or, in terms of some other pairs of the variables,

$$M(H,\tau,R) = R^{\beta/\nu r_H} m_{2H}(HR^{-\beta\delta/\nu r_H}, \tau R^{-1/\nu r_H}), \tag{34}$$

$$M(t,\tau,H) = H^{1/\delta} m_{3H}(tH^{\nu z/\beta\delta}, \tau H^{-1/\beta\delta}), \tag{35}$$

$$M(t,\tau,R) = t^{-\beta/\nu z} m_{4H}(Rt^{r_H/z}, \tau t^{1/\nu z}), \tag{36}$$

as only two out of the trio t, R, and H are independent, where all m_{iH}s are scaling functions. Equations (33) to (36) are the finite-time scaling analogues of (3).

We have therefore justified the finite-time scaling. It is remarkable in this formulation that the critical exponents are naturally identical with the usual infinite time systems'. Also, no new independent exponent has to be introduced. In fact, since an expansion of the partition function in terms of a space-time dependent magnetic field generates correlation functions, the scaling properties of thermodynamic functions of a time-dependent magnetic field such as (33) and (34) follow naturally once the field is so small that the system still remains in the critical region.

2.1.2 Theory of temperature driving

In this case, H keeps zero, but T or τ varies with time linearly. The scaling form can be derived following the procedure in the last section and can also be found in (Zhong, 2006). Here, we present an alternative semi-phenomenological derivation.

From Section 2.1.1, one can write directly the renormalization-group equation for the temperature driving as

$$\left(\mu\partial_\mu + \varsigma t\partial_t + \beta\partial_u + \gamma_{\varphi^2}\tau\partial_\tau + \frac{1}{2}\gamma\right) M = 0, \tag{37}$$

whose solution at the fixed point, Equation (24), is

$$M(t,\tau,u,\mu) = \rho^{\gamma^*/2} M(t\rho^{\varsigma^*}, \tau\rho^{\gamma^*_{\varphi^2}}, u^*, \mu\rho), \tag{38}$$

where we have directly used t in place of λ. However, as R is also a parameter, we may also write the renormalization-group equation as

$$\left\{\mu\partial_\mu + \varsigma t\partial_t + \beta\partial_u + \gamma_{\varphi^2}\tau\partial_\tau + r[u(\mu)]R\partial_R + \frac{1}{2}\gamma\right\} M = 0, \tag{39}$$

where we have assumed an additional Wilson function $r(u)$ from a new renormalization factor associated with R. Its solution at the fixed point, Equation (24), is then

$$M(t,\tau,R,u,\mu) = \rho^{\gamma^*/2} M(t\rho^{\varsigma^*}, \tau\rho^{\gamma^*_{\varphi^2}}, R\rho^{r^*}, u^*, \mu\rho), \tag{40}$$

where $r^* = r(u^*)$. Combining with the homogenous equation from dimensional analysis, Equation (27), results in

$$M(t,\tau,R,u,\mu) = \rho^{\beta/\nu} M(t\rho^z, \tau\rho^{-1/\nu}, R\rho^{-r_T}, u^*, \mu) \tag{41}$$

similar to Equation (28) with the exponents defined in Equation (30) and $r_T = 4 - r^*$ since the naïve dimension of R is 4. However, because $R = \tau/t$, only the latter two variables are independent. As a consequence,

$$\partial_t f(t,\tau) = (\partial_t - \tau/t^2\partial_R)w(t,\tau,R), \qquad \partial_\tau f(t,\tau) = (\partial_\tau + 1/t\partial_R)w(t,\tau,R) \tag{42}$$

for two arbitrary derivable functions f and w. Substituting the derivative operators in Equation (42) into (37) and comparing with (39), one finds that

$$r(u) = \gamma_{\varphi^2}(u) - \varsigma(u). \tag{43}$$

Therefore, at the fixed point, Equation (24), one has a scaling law

$$r_T = 4 - r^* = 4 - \gamma_{\varphi^2}(u^*) + \varsigma(u^*) = z + 1/\nu \tag{44}$$

using Equation (30a). Equation (44) can of course be derived as in Section 2.1.1 from a length scaling version of Equation (41),

$$M(t, \tau, R) = b^{-\beta/\nu} M(tb^{-z}, \tau b^{1/\nu}, Rb^{r_T}), \tag{45}$$

which implies

$$t' = tb^{-z}, \qquad \tau' = \tau b^{1/\nu}, \qquad R' = Rb^{r_T}, \tag{46}$$

relating variables before and after a length rescaling of factor b and $\tau = Rt$ (Zhong, 2006). From Equation (45), finite-time scaling form for the temperature driving can be derived (Zhong, 2006) as

$$M(\tau, R) = R^{\beta/\nu r_T} m_{1T}(\tau R^{-1/\nu r_T}). \tag{47}$$

Similarly, finite-time scaling forms for the non-equilibrium susceptibility and specific heat that are defined respectively as the fluctuations of the order parameter and the energy E like their equilibrium counterparts are

$$\chi(T, R) = R^{-\gamma/\nu r_T} m_{2T}(\tau R^{-1/\nu r_T}), \tag{48}$$

$$C(T, R) = R^{-\alpha/\nu r_T} m_{3T}(\tau R^{-1/\nu r_T}). \tag{49}$$

2.2 Crossover

We analyze the crossover between the regime of finite-time scaling and that of equilibrium in this section.

2.2.1 Field driving

In the case of field driving, the finite-time scaling regime is defined by

$$\tau R^{-1/\nu r_H} \lesssim 1, \qquad \tau H^{-1/\beta\delta} \lesssim 1, \qquad \tau t^{1/\nu z} \lesssim 1. \tag{50}$$

Note that

$$|\tau|^{\nu r_H} = |\tau|^{\nu z} |\tau|^{\beta\delta} \propto \xi_\infty^{-z} M_{eq}^{\delta} \propto H_{eq}/t_{eq} \equiv R_{eq} \tag{51}$$

using Equations (5), (6), and (32), where H_{eq} is an equilibrium magnetic field corresponding to an equilibrium magnetization M_{eq} at $\tau < 0$ and R_{eq} is an equilibrium rate. Equation (50) implies just

$$R \gtrsim R_{eq}, \qquad H \gtrsim H_{eq}, \qquad t \lesssim t_{eq}, \tag{52}$$

respectively. Accordingly, the finite-time scaling regime is characterized by an external rate and field that are larger than their corresponding intrinsic ones and an external time that is shorter than the intrinsic one and thus all these external scales become relevant similar to the case of finite-size scaling. As they all originate from the external driving, it is therefore reasonable and simpler to say that the finite-time scaling regime is characterized by an effective time scale R^{-1} shorter than the equilibrium correlation time t_{eq}. While in the reverse cases, for large $\tau R^{-1/\nu r_H}$ or small $R \ll R_{eq}$ for instance, the field varies so slowly that although it is changing, before it changes, the system has already equilibrated so that the usual equilibrium scaling

$$M(\tau, H) = \tau^{\beta} f_4(H\tau^{-\beta\delta}) \tag{53}$$

emerges. Therefore, the scaling functions m_{iH} have a similar asymptotic behavior as,

$$m_i(x, y) \to \begin{cases} m_{5H}(x), & \text{for } y \to 0, \\ y^{\beta} f_4(xy^{-\beta\delta}), & \text{for } y \to \infty, \end{cases} \quad (i = 1, 2, 3, 4). \tag{54}$$

The crossover occurs when $R \sim R_{eq}$ or $H \sim H_{eq}$ or $t \sim t_{eq}$.

Although the finite-time scaling regime is defined by a large R, for too large R corresponding to a large H and short t, on the other hand, the system under such a driving is too far away from equilibrium and may enter another regime.

2.2.2 Temperature driving

In this case, there is only one scaled argument, $\tau R^{-1/\nu r_T}$, in the scaling functions. The finite-time scaling regime is thus defined by the smallness of this argument, viz., $|\tau| R^{-1/\nu r_T} \lesssim 1$, or,

$$|\tau|^{-\nu r_T} R = |\tau|^{-\nu z} |\tau|^{-1} R \propto \xi_{\infty}^{z} R/|\tau| \propto t_{eq} R/|\tau| \gtrsim 1, \tag{55}$$

where Equations (5), (6), and (44) have been used. The last part of Equation (55) expresses clearly that the finite-time scaling regime is correctly defined by an effective time scale R^{-1} that is far shorter than the equilibrium correlation time t_{eq}. Accordingly, in close similarity to finite-size scaling, in this regime, the relevant scale is $\tau R^{-1}/t_{eq} = R_{eq}/R$. In the other extreme, the external time scale is so longer than t_{eq} that although the temperature is changing, before it changes, the system has already equilibrated in a way that the usual equilibrium behavior $M \propto \tau^{\beta}$ emerges independent of R. Therefore, all the scaling functions m_{iT} behave asymptotically as

$$m_{iT}(x) \to \begin{cases} \text{constant} & \text{for } x \to 0, \\ x^{\beta} & \text{for } x \to \infty, \end{cases} \quad (i = 1, 2, 3). \tag{56}$$

The crossover occurs near $\tau R^{-1} \sim t_{eq}$.

2.3 Corrections to scaling

So far, we have only considered the relevant variables such as H and τ. If there exist irrelevant variables, then there will be corrections to scaling induced by them (Wegner, 1972). We shall briefly discuss this issue in this section.

Assume that the leading irrelevant variable is Y and its corresponding exponent $\omega > 0$, Equation (45), for instance, is modified to

$$M(T, R, Y) = b^{-\beta/\nu} M(\tau b^{1/\nu}, R b^{r_T}, Y b^{-\omega}) \tag{57}$$

by neglecting the dependent variable t. Accordingly, Equation (47) becomes

$$M(T, R, Y) = R^{\beta/\nu r_T} m_{4T}(\tau R^{-1/\nu r_T}, Y R^{\omega/r_T}). \tag{58}$$

So, even at $\tau = 0$,

$$M(T_c, R, Y) = R^{\beta/\nu r_T} m_{5T}(Y R^{\omega/r_T}). \tag{59}$$

It is the scaling function m_{5T} that induces the leading algebraic corrections to scaling (Wegner, 1972). Exactly at the critical point, $R = 0$ and the corrections disappear; while near it, one can expand $m_{5T}(x)$ at $x = 0$ as a series of $x = YR^{\omega/r_T}$,

$$M(T_c, R, Y) = R^{\beta/\nu r_T}(A_0 + A_1 YR^{\omega/r_T} + A_2 YR^{2\omega/r_T} + ...), \tag{60}$$

where A_i are constants.

From Equations (1) and (11), one can also write down the scaling forms with corrections as

$$M(T, L, Y) = L^{-\beta/\nu} f_5(\tau L^{1/\nu}, YL^{-\omega}), \tag{61}$$

$$M(T, t, Y) = t^{-\beta/\nu z} f_{5t}(\tau t^{1/\nu z}, Yt^{-\omega/z}) \tag{62}$$

for finite-size scaling and short-time critical dynamics, respectively. One finds therefore that the correction-to-scaling exponent decreases sequentially from finite-size scaling (ω), to short-time critical dynamics (ω/z), and to finite-time scaling (ω/r). This implies the corrections vary quite gently in the latter as compared to the other two cases and may thus be ignored without large errors in the first approximations in estimating critical properties.

In addition, if there is a marginal variable (Wegner, 1972), logarithmic corrections to scaling appears. Finite-time scaling forms in the presence of logarithmic corrections can also be derived. We leave this for future publications.

2.4 Combined finite-time and finite-size scalings

Up to now in our discussions of finite-time scaling, we have implicitly assumed that the system size is infinite, i.e., in the thermodynamic limit. We now take the finite-size effects into account.

In this case, the transformation law for the order parameter in temperature driving, for example, is

$$M(T, R, L) = b^{-\beta/\nu} M(\tau b^{1/\nu}, Rb^{r_T}, L^{-1}b), \tag{63}$$

from which the finite-time and finite-size scaling form

$$M(T, R, L) = R^{\beta/\nu r_T} m_{6T}(\tau R^{-1/\nu r_T}, L^{-1}R^{-1/r_T}) \tag{64}$$

follows. There are then several consequences that can be drawn.

First, the regime of finite-time scaling is further restricted to $L^{-1}R^{-1/r_T} << 1$ or $R^{-1/r_T} << L$ besides $\tau R^{-1} < t_{eq}$ from Equation (55). So, for sufficiently large lattice sizes, the finite-size effects can be ignored. For not so large lattice sizes but still in the finite-time scaling regime, there are corrections from the finite size. Yet, as $L^{-1}R^{-1/r_T} << 1$, the corrections may still be small and be neglected.

Second, for $L^{-1}R^{-1/r_T} >> 1$ but $\tau R^{-1/\nu r_T} = \tau L^{1/\nu}(L^{-1}R^{-1/r_T})^{1/\nu} << 1$ or $L << \tau^{-\nu} \propto \xi_\infty$, the system then crossovers to the finite-size scaling regime.

Third, if $\tau R^{-1/\nu r_T} >> 1$ besides $L^{-1}R^{-1/r_T} >> 1$, equilibrium follows.

Combining the above three cases, one finds that the scaling function m_{6T} behaves asymptotically as

$$m_{6T}(x, y) \to \begin{cases} m_{1T}(x), & \text{for } y \to 0 \,\&\, x \to 0, \text{ finite time scaling} \\ y^{\beta/\nu} f_1(xy^{-1/\nu}), & \text{for } y \to \infty \,\&\, x \to 0, \text{ finite size scaling} \\ x^\beta, & \text{for } y \to \infty \,\&\, x \to \infty, \text{ equilibrium} \end{cases} \tag{65}$$

with the scaling functions m_{1T} and f_1 defined above in Equations (47) and (3a), respectively.

The crossover from finite-time scaling to finite-size scaling regime occurs near $R^{-1/r_T} \sim L$ for sufficiently small τ. In fact, the former regime can be regarded as an effective finite-size scaling regime in which the driving-induced effective length scale R^{-1/r_T} dominates L. This can be generalized to the concept of driving simulations by which other scalings that one needs or wants or may be difficult to consider can be simulated with driving-induced effective scales.

3. Methods of finite-time scaling

Currently, there are mainly two catalogs of methods that have been developed to estimate both static and dynamic critical exponents as well as the critical temperature on the basis of finite-time scaling. They are respectively based on the field driving and the temperature driving. The main point underlying the classification is that in the field driving, one has two variables, τ and H, at ones disposal, while in the temperature driving, only τ is at hand. As a result, to obtain all the critical exponents, one has to resort to other methods like Monte Carlo renormalization group. Of course, methods that combine some or all of these are possible. For example, the field driving with an extended dynamic Monte Carlo renormalization-group method was first applied to the first-order phase transitions in the two-dimensional Ising model (Zhong, 2002). Also, combining finite-time scaling with finite-size scaling may be helpful.

3.1 Field-driving method

This method is based on Equation (34) (Gong et al., 2010; Huang et al., 2010). In the finite-time scaling regime, the external time scale dominates and drives the system off equilibrium. Hysteresis then emerges even at T_c. In order to deal with the situation of two variables in Equation (34), we scan H back and forth with the same rate R to form a hysteresis loop and integrate over H to get its area $A = \oint MdH$. We then obtain from Equation (34) finite-time scaling forms of the coercivity H_c at $M = 0$, A, and its derivative as,

$$H_c(\tau, R) = R^{n_H} m_{6H}(\tau R^{-1/\nu r_H}), \tag{66a}$$

$$A(\tau, R) = R^{n_{aH}} m_{7H}(\tau R^{-1/\nu r_H}), \tag{66b}$$

$$\partial A(\tau, R)/\partial\tau = R^{a_1} m_{8H}(\tau R^{-1/\nu r_H}), \tag{66c}$$

with

$$n_H = \beta\delta/\nu r_H, \qquad n_{aH} = \beta(\delta+1)/\nu r_H, \qquad a_1 = \beta(\delta+1)/\nu r_H - 1/\nu r_H. \tag{67}$$

At $\tau = 0$, exact power laws

$$H_c(0, R) \propto R^{n_H}, \qquad A(0, R) \propto R^{n_{aH}}, \qquad \partial A(0, R)/\partial\tau \propto R^{a_1} \tag{68}$$

follow, from which n_H, n_{aH}, and a_1 can be determined. The critical temperature can also be determined by finding the temperature at which minimum deviations from the power law behavior, Equation (68), occurs from studying Equations (66). Combining the exponents found with the hyperscaling law $\beta(\delta+1) = d\nu$ from Equation (4), one can calculate all the static and dynamic critical exponents from

$$\begin{gathered}\delta = n_H/(n_{aH} - n_H), \quad \beta/\nu = d(n_{aH} - n_H)/n_{aH}, \quad z = d(1 - n_H)/n_{aH}, \quad r_H = d/n_{aH}, \\ \beta = (n_{aH} - n_H)/(n_{aH} - a_1), \qquad \nu = n_{aH}/d(n_{aH} - a_1).\end{gathered} \tag{69}$$

Note that in Equations (69) the first line requires only n_H and n_{aH}, while the last line needs a_1, which usually has a large statistical error due to numerical derivatives.

Of course, other observables such as χ (Huang et al., 2010) may also be employed.

The hysteresis critical exponents n_H and n_{aH} (or the rate exponent $r_H = d/n_{aH}$) have a particular meaning. Due to the scaling laws, Equations (4) and (30b), usually two critical exponents suffice to determine others for equilibrium critical phenomena. However, as δ is directly related to η via Equation (30b), knowing these two can only produce ratios of exponents instead of individual exponents, because

$$(\gamma/\nu) = (\beta/\nu)(\delta - 1), \tag{70a}$$

$$(\gamma/\nu) = 2 - \eta, \tag{70b}$$

$$2(\beta/\nu) + (\gamma/\nu) = d. \tag{70c}$$

In fact, these two exponents can be used to characterize the so-called 'weak' universality class in which exponent ratios instead of exponents themselves are identical (Suzuki, 1974). If dynamics is taken into account, one then needs z besides those two because in the usual critical dynamics, z is independent of the static ones. However, owing to the new scaling law, Equation (32), in the finite-time scaling, they are related. One can easily find indeed that n_H and n_{aH} (or r_H) suffice to determine δ, η, and z.

3.2 Temperature-driving method: Finite-time scaling with Monte Carlo renormalization group

This method is based on Equation (47) for a temperature sweep. However, it can at best give rise to the exponent ratios and T_c. In order to obtain more information, one way is to combine it with an extended dynamic Monte Carlo renormalization-group approach (Zhong, 2002). This approach may be regarded as a direct realization of Equation (46). It consists in matching correlation functions on different-sized lattices at different levels of renormalization to obtain renormalization-group eigenvalues and hence associated exponents. As a method to estimate the blocked variables, one resorts to a nearest-neighbor correlation function G_{nn} defined on a system of size Lb and assumes that after one block, it exactly matches that of a smaller system of size L without blocked, viz.,

$$G'_{nn,Lb}(T'_p, R') = G_{nn,L}(T_{ps}, R_s), \tag{71}$$

where T_p is the temperature at the peak of G_{nn} and s indicates quantities on the small lattice. In other words, one identifies the blocked variables with their unblocked counterparts on the small lattice. Consequently, one finds

$$r_T = \log(R_s/R)/\log b, \qquad \nu = \log b/\log(\tau_{ps}/\tau_p) \tag{72}$$

from Equation (46) and hence z from Equation (44). Moreover, as the two systems whose G_{nn}s are compared have the same size, size effects are thus reduced.

Iterating this blocking procedure produces a series of exponents which should be invariant after a couple of blockings that iterate away the irrelevant variables if there is a fixed point controlling the scaling behavior, because the correlation functions will then track each other.

Furthermore, combining the first two equations of Equation (46) at T_p, one finds an invariant constant

$$a \equiv \left(\frac{\tau_p}{R^{1/\nu r_T}}\right)' = \frac{\tau_p}{R^{1/\nu r_T}} \propto \left(\frac{\tau_p R^{-1}}{t_{eq}}\right)^{1/\nu r_T} \tag{73}$$

under rescaling, which reflects again the similarity with finite-size scaling in which the ratio of the correlation length $\xi_L(T_c)$ of a system of size L at T_c to L, $\xi_L(T_c)/L$, is scale invariant (Amit & Martin-Mayor, 2005). Therefore,

$$T_p = T_c + aR^{1/\nu r_T}, \tag{74}$$

which offers both a method to estimate T_c and also a consistent check of the hysteresis exponents $1/\nu r_T$ with that derived from Equation (72). Equation (74) is reasonable because at $R = 0$, or equilibrium, the correlation function ought to exhibit a peak at T_c. At a finite-time scale R^{-1}, there is an overshoot or hysteresis embodied in T_p due to the driving out of equilibrium.

The fitting and the Monte Carlo renormalization-group method then provide T_c, ν, r_T, and z. Like the case of field driving, there is a scaling law, Equation (44), relating the static exponent ν to dynamic ones r_T and z. As a result, verifying one out of the three then verifying the other two since there is a consistent check of the correctness of $1/\nu r_T$. In order to obtain other exponents, one can invoke the finite-time scaling forms of the order parameter, Equation (47), and other observables such as the non-equilibrium susceptibility, Equation (48), and specific heat, Equation (49), all of which can be measured during the course of heating without the need for independent setups. As the arguments of the scaling functions m_{iT} have been known, one can then just adjust one exponent in each case to collapse the curves of various Rs or fit M or χ or C at $\tau = 0$ or at their respective peaks if available similar to Equation (68) to obtain directly the corresponding exponents.

As a lot of critical exponents can be obtained independently, one can then test the scaling laws, Equations (4) and (70). This is important for two reasons. First, the scaling laws may be broken in some cases (Fisher, 1986; Grinstein, 1976) in which there is a dangerous irrelevant variable (Wegner, 1972). Second, if valid, they give strong evidences for the asymptotic nature of the exponents obtained which is not easily obtainable in disordered systems, because asymptotic exponents ought to satisfy scaling laws if they are valid.

4. Summary of results from finite-time scaling

We summarize briefly in this section the main results that have been obtained using the methods of finite-time scaling presented in Section 3. We again present them according to the classification we adhered to in this chapter.

4.1 Results obtained using field-driving method

The field-driving method has been applied successfully to the two-dimensional and three-dimensional Ising models (Gong et al., 2010) and the two-dimensional three- and four-state Potts models (Huang et al., 2010).

4.1.1 Simulation details

For the Ising model (Ising, 1925) in the presence of an external field, there is an inversion symmetry, which also reflects in the hysteresis loops. The coercive field can then be simply

d	n_{aH}	n_H	a_1	r_H	δ	z	β	ν
2	0.4965(18)	0.4653(19)	0.244(7)	4.028(15)	14.9(1.3)	2.154(11)	0.124(10)	0.983(28)
	$0.49487(15)^{\dagger}$	$0.46394(14)^{\dagger}$	$0.24743(8)^{\dagger}$	$4.0415(12)^{\dagger}$	$15^{\ddagger}$	$2.1665(12)^{\S}$	$1/8^{\ddagger}$	$1^{\ddagger}$
3	0.6650(28)	0.5466(22)	0.314(7)	4.511(19)	4.62(15)	2.045(13)	0.337(11)	0.632(13)
	$0.6647(6)^{\dagger}$	$0.5499(5)^{\dagger}$	$0.3131(6)^{\dagger}$	$4.513(4)^{\dagger}$	$4.789(2)^{\flat}$	$2.031(3)^{\natural}$	$0.3265(3)^{\flat}$	$0.6301(4)^{\flat}$

Table 1. Measured and derived exponents of the Ising model. †: calculated from other exponents in the same row (Zhong, 2006); ‡: exact results; §: from (Nightingale & Blöte, 1996) (Nightingale & Blöte, 2000); $^{\flat}$: from (Pelissetto & Vicari, 2002); and $^{\natural}$: average of the values estimated by (Grassberger, 1995) and (Kikuchi & Ito, 1993).

defined as in Section 3.1. In the case of the q-state Potts model (Potts, 1952), we apply an external field along one Potts state. No inversion symmetry in the hysteresis loops exist any more. We then employ the peak of a non-equilibrium susceptibility as a definition of the coercivity. Periodic boundary conditions are applied throughout. We choose several temperatures around the critical point of a model and a series of rates at each temperature. There are several considerations for the rates chosen. First, they cannot be too large to avoid far away from equilibrium, which may be qualified when the equilibrium equation of state away from the transition region is followed. Second, they cannot be too small to avoid leaving the finite-time scaling regime for the equilibrium or finite-size scaling regime. Third, they should be as small as possible in order to reduce errors from the relatively large values of an observable at large rates as compared to the small ones. Then, for each chosen temperature and rate, we start a Monte Carlo simulation at an ordered state with a sufficiently large external field that is larger than the closure field of the hysteresis loops at that rate to ensure closure of the loops and that has otherwise been checked to have no effect on the results. Several Monte Carlo steps suffice to equilibrate the system as it is far away from its critical point. After equilibrium, the field is swept with the rate back and forth for 100 times, say, to obtain 100 hysteresis loops. Averaged values of A and M can then be obtained. The method presented in Section 3.1 then yields T_c and exponents.

4.1.2 Results

The T_cs for both models determined from the minimum deviations of A from pure power laws agree well with their respective exact results. Knowing T_c can then give rise to the critical exponents, which are given in Tables 1 (Gong et al., 2010) and 2 (Huang et al., 2010). One sees that the present results agree reasonably well with the exact ones, showing the effectiveness of the method. Note that besides the early real-space renormalization-group studies (see (Wu, 1982) for a review), the present is the one that directly applies an external field to estimate δ, though it can also be estimated by other critical exponents through scaling laws. Slightly overlapped within the statistical errors as they are, our δs for $q = 3$ and 4 still support their respective conjectured values. The dynamic critical exponent zs obtained for both the $q = 3$ and $q = 4$ Potts model agree well with previous Monte Carlo simulation results (de Alcantara Bonfim, 1987; Tang & Landau, 1987). Along with z in Table 1 of the two-dimensional Ising model that is equivalent to the $q = 2$ Potts model, they appear to confirm the dynamic weak universality (de Alcantara Bonfim, 1987; Tang & Landau, 1987) according to which the Potts model with $q = 2$, $q = 3$, and $q = 4$ all share the same z. However, they are apparently distinct from the short-time dynamic results of $z = 2.29$ for $q = 4$ (da Silva et al., 2002; Fernandes et al., 2006) but $z = 2.19$ for $q = 3$ (da Silva et al., 2002; Okano et al., 1997; Zhang et al., 1999). Thus, further studies are still needed here.

q	n_{aH}	n_H	a_1	r_H	δ	β/ν	β	ν	z
3	0.4969(12)	0.4624(9)	0.200(10)	4.025(10)	13.4(6)	0.139(6)	0.116(5)	0.838(3)	2.164(7)
	0.4962(8)‡	0.4631(8)‡	0.1985(10)‡	4.031(7)‡	14†	2/15†	1/9†	5/6†	
4	0.4954(13)	0.4645(21)	0.154(12)	4.039(11)	15.1(1.3)	0.124(10)	0.0900(7)	0.726(3)	2.163(10)
	0.4953(12)‡	0.4643(11)‡	0.1238(15)‡	4.038(10)‡	15†	1/8†	1/12†	2/3†	

Table 2. Measured and derived exponents of the two-dimensional Potts model. †: conjectured values (Wu, 1982); ‡: calculated from the conjectured values and the measured zs.

4.2 Results obtained using temperature-driving method

This method has been applied successfully to pure systems including the two-dimensional Ising model (Zhong & Xu, 2005) and the three-state Potts model (Fan & Zhong, 2007), and disordered systems including a two-dimensional random-bond Potts model with the state number $q = 5$ and $q = 8$ (Fan & Zhong, 2009), a three-dimensional random-bond Ising model (Xiong et al., 2010a), and a three-state random-bond Potts model (Xiong et al., 2010b).

4.2.1 Simulation details

In this case, in addition to the general considerations and boundary conditions given in Section 4.1.1, a pair of lattice sizes, for example, 128 and 64 in three dimensions has to be used owing to the two-lattice matching in renormalization. For a given R and, in the case of disordered systems, a disorder strength and a sample of its fixed realization, we start a Monte Carlo simulation from a completely ordered state at an initial temperature that is chosen to be so far away from T_p that it has been checked to have no effect on the results. After one time unit consisting of a sequential sampling of all the spins with the usual Metropolis algorithm (Metropolis et al., 1953), T is increased by R. The system then evolves with time until a disordered state is reached. At each time in the course of heating, we calculate a sample of M, G_{nn}, and E and perform sequentially blockings on the configurations from which the renormalized G_{nn} is computed by means of a majority rule with $b = 2$. Ties are broken by a random selection among the tied states. Each quantity is then averaged at each time step over different samples.

4.2.2 Results

So far, the critical temperatures obtained agree quite well with either exact results (Fan & Zhong, 2007; 2009; Zhong & Xu, 2005) or existing estimates (Fan & Zhong, 2009; Xiong et al., 2010b) or an approximate theory (Xiong et al., 2010a;b). The critical exponents obtained for the pure two-dimensional Ising model, $\nu = 0.97(8)$, $z = 2.15(13)$, and $\beta = 0.12(1)$ for only 8 to 40 samples, and for the pure two-dimensional three-state Potts model, $\nu = 0.816(27)$, $z = 2.171(62)$ and $\beta = 0.108(4)$ for more than 200 samples and hence smaller statistical errors, agree well with the corresponding values listed in Tables 1 and 2. A positive $\alpha = 0.368(54)$ calculated from the hyperscaling law, Equation (4a), has also been testified by a scaling collapse of the specific heat curves for the latter model (Fan & Zhong, 2007).

Disorder is ubiquitous; its effects on critical behavior are thus important. This has become clear from Harris criterion (Cardy, 1996; Harris, 1974), namely, uncorrelated quenched randomness coupled to local energy density is irrelevant and the universality class of the pure system persists when its specific heat critical exponent $\alpha < 0$, while such randomness will lead to a new universality class controlled by a new 'random' fixed point when $\alpha > 0$. To identify the asymptotic critical exponents that characterize the random fixed point in the latter case is, however, not a simple task, as disorder-dependent critical exponents are frequently obtained, possibly reflecting the competition of different fixed points (Berche & Chatelain,

r_0	q	r_T	ν	$1/\nu r_T$	z	β	β/ν	$\alpha = 2 - d\nu$
3	8	4.39(12)	0.757(43)	0.302(16)	3.07(12)	0.130(15)	0.172(10)	0.49(9)
	5	4.15(8)	0.818(43)	0.295(13)	2.93(7)	0.128(10)	0.157(4)	0.36(9)
10	8	5.43(13)	1.021(35)	0.181(7)	4.45(13)	0.170(20)	0.167(14)	-0.042(70)
	5	5.12(7)	1.027(23)	0.190(5)	4.15(7)	0.161(20)	0.157(16)	-0.054(46)
15	8	5.75(15)	1.098(27)	0.158(6)	4.84(15)	0.173(20)	0.158(14)	-0.196(54)
	5	5.44(10)	1.112(34)	0.167(5)	4.54(9)	0.164(20)	0.148(14)	-0.22(7)
20	8	5.88(17)	1.180(35)	0.144(5)	5.03(17)	0.176(20)	0.149(13)	-0.36(7)
	5	5.62(14)	1.182(34)	0.151(5)	4.77(14)	0.170(20)	0.144(13)	-0.36(7)

Table 3. Critical exponents of the two-dimensional random-bond Potts model.

r_0	r_T	ν	$1/\nu r_T$	z	β	α	γ	β/ν	γ/ν
2	3.60(6)	0.651(18)	0.427(7)	2.061(32)	0.374(6)	−0.035(16)	1.389(18)	0.575(18)	2.13(7)
4	3.57(5)	0.682(18)	0.410(7)	2.108(35)	0.349(6)	−0.046(17)	1.330(22)	0.512(16)	1.95(7)
5	3.57(5)	0.689(18)	0.407(7)	2.119(37)	0.343(6)	−0.052(17)	1.333(22)	0.498(16)	1.93(7)
10	3.48(5)	0.765(19)	0.376(6)	2.175(35)	0.354(6)	−0.130(29)	1.420(32)	0.463(17)	1.86(5)

Table 4. Critical exponents of the three-dimensional random-bond Ising model.

r_0	r_T	ν	$1/\nu r_T$	z	β	α	γ	β/ν	γ/ν
2.5	4.28(3)	0.518(11)	0.451(7)	2.38(3)	0.206(8)	0.54(2)	1.16(2)	0.40(2)	2.24(6)
5	4.30(4)	0.540(9)	0.431(6)	2.44(3)	0.25(2)	0.48(3)	1.15(2)	0.46(4)	2.13(5)
7.5	4.32(5)	0.542(10)	0.426(6)	2.47(4)	0.29(3)	0.40(3)	1.15(2)	0.54(6)	2.12(5)
10	4.31(5)	0.554(9)	0.419(6)	2.51(4)	0.30(3)	0.36(3)	1.15(3)	0.54(6)	2.08(7)
15	4.34(6)	0.566(15)	0.408(7)	2.57(3)	0.31(3)	0.29(4)	1.15(5)	0.55(6)	2.03(10)
20	4.34(7)	0.569(16)	0.406(9)	2.58(5)	0.32(3)	0.28(4)	1.15(5)	0.56(6)	2.02(12)
30	4.21(11)	0.673(25)	0.353(9)	2.72(8)	0.34(4)	0.27(4)	1.25(5)	0.51(6)	1.86(10)

Table 5. Critical exponents of the three-dimensional three-state random-bond Potts model.

2004; Folk et al., 2003). We have studied three random-bond models in which the single pure bonds can randomly select between a weak bond K and a strong one r_0K with equal probability with r_0 characterizing the disorder strength. The three-dimensional random-bond Ising model in its pure version has a continuous transition with a positive α, while the two- and three-dimensional Potts models studied have first-order phase transitions in their pure version and disorders make them continuous (Aizenman & Wehr, 1989; Cardy & Jacobsen, 1997; Hui & Berker, 1989). All the three models will thus exhibit new universality classes in principle.

The exponents obtained using the method detailed in Section 3.2 of the three models are listed in Tables 3 to 5. They have been checked to be independent of the lattice sizes used for some disorder strengths in all the models. Generally speaking, our exponents agree quite well with existing results except ν and α of the latter model (Xiong et al., 2010b). Details can be found in the original papers and we shall not discuss them here to save space. Rather, we shall only focus on those special aspects.

For the two-dimensional random-bond Potts model, its exponents in Table 3 exhibit two distinct regimes with α showing opposite signs, which, as indicated, is calculated by the scaling law, Equation (4a), and has been checked by scaling collapses. A positive α means $\nu < 1$ as seen, which violates the bound

$$\nu \geq 2/d \tag{75}$$

suggested to be satisfied for disordered systems (Chayes et al., 1986). This violation was also found in (Cardy & Jacobsen, 1997) but was later argued to be due to the insufficient disorder strength because for $q \gtrsim 2$ it was found that the bound (75) was satisfied for stronger disorders in agreement with our results, suggesting the violation was a result of crossover from the pure fixed point to the random fixed point (Jacobsen, 2000). However, in our case, $q > 4$ and the pure model exhibits a discontinuous rather than a continuous transition. Although the hyperscaling law, Equation (4a), has been testified in this case and hence the activated dynamics proposed originally for the random-field Ising model (Fisher, 1986) is excluded (Deroulers & Young, 2002), as no further exponents have been obtained, one cannot draw definite conclusions about this regime. For $q = 8$, $r_0 \sim 10$ was found to be close to the random fixed point (Cardy & Jacobsen, 1997) and our β/ν of $r_0 = 10$ appears to be a little larger than $0.142(1)$ (Cardy & Jacobsen, 1997), $0.153(3)$ (Chatelain & Berche, 1998), and $0.153(1)$ (Jacobsen & Picco, 2000). Yet, $r_0 = 8$ to 20 was found to locate the random fixed point with $\beta/\nu = 1.50$ to 1.55 (Picco, 1998). If we averaged the three values within this range, we would get $\beta/\nu = 1.58(8)$ that would agree quite well with those quoted values and also with $0.157(2)/0.156(11)$ of short-time critical dynamics (Yin et al., 2004). The same average yields $\nu = 1.100(19)$ which appears again a little larger than about 1.02 (Cardy & Jacobsen, 1997; Chatelain & Berche, 1998). However, ν was found to increase slightly with q with the $q = 3$ value of $1.02(2)$ (Jacobsen, 2000). So, a slightly larger ν for larger q may be still possible. We may also consider averages over $r_0 = 15$ and 20 whose exponents appear closer in value. Anyway, the true critical exponents for the random fixed point in this model still need further studies.

The three-dimensional disordered Ising model as a paradigm of a positive α in the pure case has attracted much interest (Folk et al., 2003) and its renormalization-group theory has reached a level of up to six loops (Pelissetto & Vicari, 2000). However, problems still exist concerning for example its true critical exponents (Xiong et al., 2010a). As a lot of exponents can be estimated, we are able to test the scaling laws as shown in Table 6. One sees that in the middle range of disorders, the exponents satisfy the three scaling laws tested and vary little. The averaged exponents within this range are thus regarded as the asymptotic critical exponents of the random fixed point. They agree well with results of other types of disorders and of the renormalization-group theory. These results thus lead to several conclusions. First, for the random fixed point, we have proved the validity of the scaling laws, which was invoked previously to reckon the correctness of the obtained exponents (Pelissetto & Vicari, 2000). Second, they help to unify the exponents. For example, our dynamic critical exponent of $z = 2.114(51)$ supports a lower value found by renormalization-group analyzes, experiments, and some Monte Carlo simulations rather than the larger values of $z \approx 2.6$ (Parisi et al., 1999; Schehr & Paul, 2005) and $z \approx 2.35$ (Calabrese et al., 2008; Hasenbusch et al., 2007). Third, they corroborate the universality of the random fixed point with respect to the form of disorders. Fourth, they show that corrections to scaling can indeed be ignored in estimating exponents in finite-time scaling. Fifth, they also demonstrate the effectiveness of finite-time scaling in probing both static and dynamic critical behavior. The exponents at $r_0 = 2$ and $r_0 = 10$ do not satisfy all scaling laws and may thus be crossover exponents that reflect crossover from the random fixed point to the pure and to the percolation fixed point, respectively. Conversely, validating of a single or even two scaling laws may not be invoked as an indication of the asymptotic nature of the obtained exponents.

The three-dimensional random-bond Potts model shows gross features that are similar to the random-bond Ising model. In particular, one finds from Table 7 that the first two scaling laws are satisfied within the errors for $r_0 \simeq 10$ to 20, and almost satisfied for $r_0 = 7.5$, but not for the other disorder strengths, while the third law can be considered as satisfied for all r_0

r_0	2	4	5	10	Exact value
$\alpha + d\nu$	1.92(6)	2.00(6)	2.01(6)	2.17(6)	2
$\alpha + 2\beta + \gamma$	2.10(3)	1.98(3)	1.97(3)	2.00(5)	2
$2\beta/\nu + \gamma/\nu$	3.28(10)	2.97(9)	2.93(8)	2.79(8)	3

Table 6. Test of scaling laws for the three-dimensional random-bond Ising model.

r_0	2.5	5	7.5	10	15	20	30	Exact value
$\alpha + d\nu$	2.09(4)	2.10(4)	2.03(4)	2.01(5)	1.97(6)	1.99(6)	2.30(9)	2
$\alpha + 2\beta + \gamma$	2.10(3)	2.13(5)	2.13(7)	2.11(7)	2.06(9)	2.07(9)	2.20(10)	2
$2\beta/\nu + \gamma/\nu$	3.04(8)	3.05(9)	3.20(13)	3.16(14)	3.13(16)	3.14(16)	2.88(18)	3

Table 7. Test of scaling laws for the three-dimensional random-bond Potts model.

studied. Therefore, conclusions similar to the Ising model can also be drawn. For example, the exponents within $r_0 \simeq 10$ to 20 are asymptotic and controlled by the random-fixed point in the model while those outside are only crossover. Corrections to scaling can again be ignored, etc.

However, there is an important difference. α for the random fixed point is positive and thus ν violates the bound (75) in contrary to recent numerical studies (Ballesteros et al., 2000; Chatelain et al., 2001; 2005; Mercaldo et al., 2005; 2006; Murtazaev et al., 2007; 2008; Yin et al., 2005; 2006) and a renormalization-group analysis (Aharony et al., 1998). In the two-dimensional random-bond Potts model, a positive α has also been found as pointed out above. However, for large disorder strengths, α becomes negative and ν satisfies the bound. In the present case, α is still a large positive number even for $r_0 = 30$, whose $\nu = 0.673(25)$ is on the verge of $2/d$ albeit with a large error. A hint for a positive α has also been found but with $\nu > 2/d$ in a three-dimensional random-bond Potts model in the large-q limit (Mercaldo et al., 2005; 2006). Yet, the author claimed that the asymptotic region for the specific heat was far from the possibilities of present-day numerical calculations (Mercaldo et al., 2005; 2006). Negative αs have been obtained on a small range of lattice sizes ($L = 20 - 44$) using finite-size scaling but without considering corrections to scaling (as the exponent is several times bigger than that of finite-time scaling, Section 2.3) and without showing scaling collapse for the three-dimensional three-state Potts model with site dilutions (Murtazaev et al., 2007; 2008). This was obtained by fitting the peaks of the specific heat to

$$C = c_1 - c_2 L^{\alpha/\nu} \tag{76}$$

for a negative α, where c_1 and c_2 are positive constants. We have found that in some ranges of rates, a fit to Equation (76) with L replaced by $R^{-1/r}$ according to Section 2.4 does give a negative α, but the C curves collapse badly even we adjust α in the negative region (Xiong et al., 2010b). On the contrary, in the case of the random-bond Ising model, fits to such a form indeed lead to those negative αs listed in Table 4, which collapse the specific curves well. In contrast, fits to the positive α forms can also yield positive αs but then the specific curves collapse badly (Xiong et al., 2010a). In addition, in the two-dimensional three-state pure Potts model, we have essentially applied the same methods to correctly identify its positive α as mentioned in the first paragraph in this section. Moreover, all exponent ratios agree well with existing ones. Furthermore, z agrees well with that from short-time critical dynamics (Yin et al., 2005). This single exponent then lends support to our ν and through Equation (4a) α as pointed out in Section 3.2. All these therefore strongly support our positive α and $\nu < 2/d$.

In fact, for a dirty system, it has been known that its stability is not directly related to its α, which may thus assume positive values (Andelman & Berker, 1984; Kinzel & Domany, 1981), though the opposite is true for a pure system according to the Harris criterion (Harris, 1974). Moreover, it has also been pointed out that for systems in which self-averaging breaks down (Aharony & Harris, 1996; Wiseman & Domany, 1995; 1998), the ν that is found by finite-size scaling and was proved to satisfied the bound (75) (Chayes et al., 1986) may be different from the intrinsic ν that might escape it, since the former is found to be only a result of the grand canonical ensemble average used (Pazmandi et al., 1997), though a renormalization-group analysis shows that the average procedure is irrelevant (Aharony et al., 1998). If this is true, finite-time scaling will be superior.

5. Conclusion

We have reviewed in this Chapter the idea, the theory, and the methods of finite-time scaling and the results of their applications to the continuous phase transitions in both pure and disordered two- and three-dimensional Ising and Potts models. Both field driving and temperature driving have been considered. Both static and dynamic critical exponents as well as the critical points can all be estimated. As a lot of exponents can be determined independently, scaling laws can be tested, which is a valuable information for reckoning the asymptotic nature of the exponents. So far, most results obtained agree quite well with those from other sources and those disagreed appear quite possibly true. If the latter is shown to be correct, finite-time scaling will be superior to finite-size scaling. Even if it were finally shown to be wrong, the former results still have already demonstrated its effectiveness; and the lessons gained would certainly push it forward. We conclude that the idea behind finite-time scaling is physically so simple and in so close analogue to that of finite-size scaling that it should at least be a useful concept in statistical physics.

To end the review, we remarks on some other advantages and disadvantages of the finite-time scaling. It is a nonequilibrium approach that drives a system out of equilibrium. As a consequence, hysteresis ensues even at T_c. It is distinct from usual approaches in that it manipulates the dynamics of a system by an external driving field or temperature. This enables it to avoid critical slowing down (Gong et al., 2010; Huang et al., 2010). As has been pointed out, the correction-to-scaling exponent is rather small compared to finite-size scaling and short-time critical dynamics. This has two sides. On the one hand, it makes estimation of exponents rather simple since the corrections appear negligible. Moreover, the error bars of the exponents so estimated are also on a par with other usual methods. On the other hand, if one wants to make more precise estimations including the correction-to-scaling exponent, large ranges of time scales appear necessary. We have so far concentrated on the local dynamics as realized in the Monte Carlo simulations of single-site Metropolis algorithm and their equivalent Langevin dynamics, the idea of finite-time scaling, however, should be applicable to other dynamics as well. Finally, we would point out that the method of linear driving may probably be the simplest but most general approach to finite-time scaling and should also be amenable to experiments (Gong et al., 2010). It may also be generalized to a concept of driving simulations (Section 2.4) that apply the linear driving to simulate other effects like system sizes near criticality.

Future studies may include applying and testing finite-time scaling in other systems including quantum ones, exploiting the combined scalings of both finite times and finite sizes, developing approaches to improve the precision of the present methods, and applying the scaling experimentally to study critical phenomena, etc. Another area that finite-time scaling is helpful is the scaling behavior in first-order phase transitions by driving (Zhang et al., 1995). In fact, the renormalization-group theory for the linear driving developed first in this area (Zhong & Chen, 2005). Moreover, the linear driving may possibly be crucial here (Fan & Zhong, 2010).

6. Acknowledgement

I am grateful to my professor, Professor Jinxiu Zhang. My use of the linear driving method originated from him. I am also indebted to my students, Zhifang Xu, Shuangli Fan, Shurong Gong, Xianzhi Huang, and Wanjie Xiong, whose practices and discussions drove me to develop the theory and methods presented here. ZX initiated simulations in the continuous transition of the Ising model. SF first considered the specific heat and WX included the susceptibility. SG first extended the renormalization-group theory to the off-critical situation. In addition, most of the numerical results presented here were obtained by them. Another student, Shuai Yin, always took part actively in our group meetings and his helpful discussions in completing the other derivation of the scaling law, Equation (44), and others are also appreciated. This work was support by the National Natural Science Foundation of China (Grant Nos. 10374118 and 10625420), the FANEDD and EYTP of MOE, China, and NSF of Guangdong Province, China (Grant No. 011140).

7. References

Aharony A. & Harris, A. B. (1996). Absence of self-averaging and universal fluctuations in random systems near critical points. *Phys. Rev. Letts.*, Vol. 77, 3700-3703.

Aharony, A.; Harris, A. B. & Wiseman, S. (1998). Critical disordered systems with constraints and the inequality $\nu > 2/d$. *Phys. Rev. Lett.*, Vol. 81, 252-255.

Aizenman, M. & Wehr, J. (1989). Rounding of first-order phase transitions in systems with quenched disorder. *Phys. Rev. Lett.*, Vol. 62, 2503-2506.

Amit, D. J.; Martin-Mayor, V. (2005). *Field Theory, the Renormalization Group, and Critical Phenomena*, 3rd edition, World Scientific, Singapore.

Andelman D. & Berker, A. N. (1984). Scale-invariant quenched disorder and its stability criterion at random critical points. *Phys. Rev. B*, Vol. 29, 2630-2635.

Ballesteros, H. G.; Fernández, L. A.; Martín-Mayor, V.; Muñoz Sudupe, A.; Parisi, G. & Ruiz-Lorenzo, J. J. (2000). Critical behavior in the site-diluted three-dimensional three-state Potts model. *Phys. Rev. B*, Vol. 61, 3215-3218.

For a review, see Berche, B. & Chatelain, C. (2004). Phase transitions in two-dimensional random Potts models. In: *Order, Disorder, and Criticality*, Holovatch, Yu. (Ed.), 147-199, World Scientific, Singapore.

Binder, K. & Heermann, D. (1988). *Monte Carlo Simulations in Statistical Physics*, Springer, Berlin.

Brézin, E. (1982). An investigation of finite size scaling. *J. de Phys.*, Vol. 43, 15-22.

Brézin, E. & Zinn-Justin. J. (1985). Finite size effects in phase transitions. *Nucl. Phys.B*, Vol. 257, 867-893.

Calabrese, P.; Pelissetto, A. & Vicari, E. (2008). Static and dynamic structure factors in three-dimensional randomly diluted Ising models. *Phys. Rev. E*, Vol. 77, 021126.

Cardy, J. (1988). *Finite Size Scaling*, (Ed.), North-Holland, Amsterdam.

Cardy, J. (1996). *Scaling and Renormalization in Statistical Physics*, Cambridge, Cambridge.

Cardy, J. & Jacobsen, J. L. (1997). Critical behavior of random-bond Potts models. *Phys. Rev. Lett.*, Vol. 79, 4063-4066.

Chayes, J. T.; Chayes, L.; Fisher, D. S. & Spencer, T. (1986). Finite-size scaling and correlation lengths for disordered systems. *Phys. Rev. Lett.*, Vol. 57, 2999-3002.

Chatelain C. & Berche, B. (1998). Finite-size scaling study of the surface and bulk critical behavior in the random-bond eight-state Potts model. *Phys. Rev. Lett.*, Vol. 80, 1670-1673.

Chatelain, C.; Berche, B.; Janke, W. & Berche, P. E. (2001). Softening of first-order transition in three-dimensions by quenched disorder. *Phys. Rev. E*, Vol. 64, 036120.

Chatelain, C.; Berche, B.; Janke, W. & Berche, P. E. (2005). Monte Carlo study of phase transitions in the bond-diluted 3D 4-state Potts model. *Nucl. Phys. B*, Vol. 719 [FS], 275-311.

da Silva, R.; Alves, N. A. & Drugowich de Felício, J. R. (2002). Mixed initial conditions to estimate the dynamic critical exponent in short-time Monte Carlo simulation. *Phys. Lett. A*, Vol. 298, 325-329.

de Alcantara Bonfim, O. F. (1987). Critical dynamics of the q-state Potts model in two dimensions. *Europhys. Lett.*, Vol. 4, 373-376.

De Dominicis, C. & Peliti, L. (1978). Field-theory renormalization and critical dynamics above T_c: Helium, antiferromagnets, and liquid-gas systems. *Phys. Rev.B* , Vol. 18, 353-376.

Deroulers C. & Young, A. P. (2002). Critical behavior and lack of self-averaging in the dynamics of the random Potts model in two dimensions. *Phys. Rev. B*, Vol. 66, 014438.

Fan, S. & Zhong, F. (2007). Determination of the dynamic and static critical exponents of the two-dimensional three-state Potts model using linearly varying temperature. *Phys. Rev. E*, Vol. 76, 041141.

Fan, S. & Zhong, F. (2009). Critical dynamics of the two-dimensional random-bond Potts model with nonequilibrium Monte Carlo simulations. *Phys. Rev. E*, Vol. 79, 011122.

Fan, S. & Zhong, F. (2010). Evidences for the instability fixed points of first-order phase transitions. submitted.

Fernandes, H. A.; Arashiro, E.; Drugowich de Felício, J. R. & Caparica, A. A. (2006). An alternative order parameter for the 4-state potts model. *Physica A*, Vol. 366, 255-264.

Ferrell, R. A.; Menyhárd, N.; Schmidt, H.; Schwabl, F. & Szépfalusy, P. (1967). Dispersion in second sound and anomalous heat conduction at the lambda point of liquid helium. *Phys. Rev. Lett.*, Vol. 18, 891-894.

Fisher, M. E. (1967). Theory of condensation and critical point. *Physics*, Vol. 3, 255-283.

Fisher, M. E. & Ferdinand, A. E. (1967). Interfacial, boundary, and size effects at critical points. *Phys. Rev. Lett.*, Vol. 19, 169-172.

Fisher, M. E. & Barber, M. N. (1972). Scaling theory for finite-size effects in the critical region. *Phys. Rev. Lett.*, Vol. 28, 1516-1519.

Fisher, D. S. (1986). Scaling and critical slowing down in random-field Ising systems. *Phys. Rev. Lett.*, Vol. 56, 416-419.

For a review, see Folk, R.; Holovatch, Yu. & Yavors'kii, T. (2003). Critical exponents of a three dimensional weakly diluted quenched Ising model. *Usp. Fiz. Nauk*, Vol. 173, 175-200 [*Phys. Usp.*, Vol. 46, 169-191].

Folk, R. & Moser, G. (2006). Critical dynamics: a field-theoretical approach. *J. Phys. A*, Vol. 39, R207-R313.

Gasparini, F. M.; Kimball, M. O.; Mooney, K. P.; & Diaz-Avila, M. (2008). Finite-size scaling of He4 at the superfluid transition. *Rev. Mod. Phys.*, Vol. 80, 1009-1059.

Glauber, R. J. (1963). Time-dependent statistics of the Ising model. *J. Math. Phys.*, Vol. 4, 294-307.

Gong, S.; Zhong, F.; Huang, X. & Fan, S. (2010). Finite-time scaling via linear driving. *New J. Phys.*, Vol. 12, 043036.

Grassberger, P. (1995). Damage spreading and critical exponents for "model A" Ising dynamics. *Physica A*, Vol. 214, 547-559.

Grinstein, G. (1976). Ferromagnetic phase transitions in random fields: The breakdown of scaling laws. *Phys. Rev. Lett.*, Vol. 37, 944-947.

Halperin, B. I. & Hohenberg, P. C. (1967). Generalization of scaling laws to dynamical properties of a system near its critical point. *Phys. Rev. Lett.*, Vol. 19, 700-703.

Harris, A. B. (1974). Effect of random defects on the critical behaviour of Ising models. *J. Phys. C*, Vol. 7, 1671-1692.

Hasenbusch, M.; Pelissetto, A. & Vicari, E. (2007). Relaxational dynamics in 3D randomly diluted Ising models. *J. Stat. Mech.*, Vol. 2007, P11009.

Hohenberg, P. C. & Halperin, B. I. (1977). Theory of dynamic critical phenomena. *Rev. Mod. Phys.*, Vol. 49, 435-479.

Huang, X.; Gong, S.; Zhong, F. & Fan, S. (2010). Finite-time scaling via linear driving: Application to the two-dimensional Potts model. *Phys. Rev. E*, Vol. 81, 041139.

Hui K. & Berker, A. N. (1989). Random-field mechanism in random-bond multicritical systems. *Phys. Rev. Lett.*, Vol. 62, 2507-2510.

Hukushima, K. & Nemeto, K. (1995). On the forced oscillator method for the eigenvalue spectrum edge of $\pm J$ random matrix. *J. Phys. Soc. Japan*, Vol. 64, 1863-1865.

Ising, E. (1925), Beitrag zur Theorie des Ferromagnetismus. *Z. Phys.*, Vol. 31, 253-258.

Jacobsen, J. L. (2000). Multiscaling of energy correlations in the random-bond Potts model. *Phys. Rev. E*, Vol. 61, R6060-R6063.

Jacobsen, J. L. & Picco, M. (2000). Large-q asymptotics of the random-bond Potts model. *Phys. Rev. E*, Vol. 61, R13-R16.

Janssen, H. K.; Schaub, B. & Schmittmann, B. (1989). New universal short-time scaling behaviour of critical relaxation processes. *Z. Phys. B*, Vol. 73, 539-549.

Janssen, H. K. (1992). On the renormalized field theory of nonlinear critical relaxation. *From Phase Transitions to Chaos*. Györgyi, G.; Kondor, I.; Sasvári, L. & Tél, T. (Ed.), World Scientific, Singapore.

Kikuchi, M. & Ito, N. (1993). Statistical dependence time and its application to dynamical critical exponent. *J. Phys. Soc. Japan*, Vol. 62, 3052-3061.

Kinzel, W. & Domany, E. (1981). Critical properties of random Potts models. *Phys. Rev. B*, Vol. 23, 3421-3434.

Landau, D. P & Binder, K. (2005). *A Guide to Monte Carlo Simulations in Statistical Physics*, 2nd edition, Cambridge University Press, Cambridge.

Li, Z. B.; Schülke, L. & Zheng, B. (1995). Dynamics Monte Carlo measurement of critical exponents. *Phys. Rev. Lett.*, Vol. 74, 3396-3399.

Ma, S. -k. (1976). *Modern Theory of Critical Phenomena*, Benjamin, New York.

Martin, P. C.; Siggia, E. D. & Rose, H. A. (1973). Statistical dynamics of classical systems. *Phys. Rev. A*, Vol. 8, 423-437.

Mercaldo, M. T.; Anglès d'Auriac, J.-Ch. & Iglói, F. (2005). Disorder-driven phase transitions of the large q-state Potts model in three dimensions. *Europhys. Lett.*, Vol. 70, 733-739.

Mercaldo, M. T.; Anglès d'Auriac, J.-Ch. & Iglói, F. (2006). Critical and tricritical singularities of the three-dimensional random-bond Potts model for large q. *Phys. Rev. E*, Vol. 73, 026126.

Metropolis, N.; Rosenbluth, A. W.; Rosenbluth, M. N.; Teller A. M. & Teller, E. (1953). Equation of state calculations by fast computing machines. *J. Chem. Phys.*, Vol. 21, 1087-1092.

Müler-Krumbhaar, H. & Binder, K. (1973). Dynamic properties of the Monte Carlo method in statistical mechanics. *J. Stat. Phys.*, Vol. 8, 1-24.

Murtazaev, A.; Kamilov, I. & Babaev, A. (2007). Investigation of the critical properties of the three-dimensional weakly diluted potts model. *Bulletin of the Russian Academy of Sciences: Physics*, Vol. 71, 1586-1588.

Murtazaev, A.; Babaev, A. & Aznaurova, G. (2008). Investigation of the influence of quenched nonmagnetic impurities on phase transitions in the three-dimensional Potts model. *Physics of the Solid State*, Vol. 50, 733-739.

Newman, M. E. J. & Barkema, G. T. (1999). *Monte Carlo Methods in Statistical Physics*, Clarendon, Oxford.

Nightingale, M. P. & Blöte, H. W. J. (1996). Dynamic exponent of the two-dimensional Ising model and Monte Carlo computation of the subdominant eigenvalue of the stochasticmatrix. *Phys. Rev. Lett.*, Vol. 76, 4548-4551.

Nightingale, M. P. & Blöte, H. W. J. (2000). Monte Carlo computation of correlation times of independent relaxation modes at criticality. *Phys. Rev. B*, Vol. 62, 1089-1101.

Okano, K.; Schulke, L.; Yamagishi, K. & Zheng, B. (1997). Universality and scaling in short-time critical dynamics. *Nucl. Phys. B*, Vol. 485 [FS], 727-746.

Parisi, G.; Ricci-Tersenghi, F. & Ruiz-Lorenzo, J. J. (1999). Universality in the off-equilibrium critical dynamics of the three-dimensional diluted Ising model. *Phys. Rev. E*, Vol. 60, 5198-5201.

Pazmandi, F.; Scalettar, R. T. & Zimanyi, G. T. (1997). Revisiting the theory of finite size scaling in disordered systems: ν can be less than $2/d$. *Phys. Rev. Lett.*, Vol. 79, 5130-5133.

Pelissetto, A. & Vicari, E. (2000). Randomly dilute spin models: A six-loop field-theoretic study. *Phys. Rev. B*, Vol. 62, 6393-6409.

Pelissetto, A. & Vicari, E. (2002). Critical phenomena and renormalization-group theory. *Phys. Rep.*, Vol. 368, 549-727.

Picco, M. (1998). A study of cross-over effects for the 2D random bond Potts model. e-print cond-mat/9802092.

Potts, R. B. (1952). Some generalized order-disorder transformations. *Proc. Cambridge. Phil. Soc.*, Vol. 48, 106-109.

(1990) *Finite Size Scaling and Numerical Simulations of Statistical Systems*, Privman, V. (Ed.), World Scientific, Singapore.

Schehr G. & Paul, R. (2005). Universal aging properties at a disordered critical point. *Phys. Rev. E*, Vol. 72, 016105.

Shima, H. & Nakayama, T. (1998). Finite-time scaling approach for the ac conductivity near the Anderson Transiiton. *J. Phys. Soc. Japan*, Vol. 67, 2189-2192.

Shima, H. & Nakayama, T. (1999). Critical behavior of ac conductivity near the Anderson transition. *Phys. Rev. B*, Vol. 60, 14066-14071.

Shinomoto, S. & Kabashima, Y. (1991). Finite time scaling of energy in simulated annealing. *J. Phys. A*, Vol. 24, L141-L144.

Stanley, H. E. (1971). *Introduction to Phase Transitions and Critical Phenomena*, Oxford, London.

Suzuki, M. (1974). New universality of critical exponents. *Prog. Theor. Phys.*, Vol. 51, 1992-1993.

Suzuki, M. (1977). Static and dynamic finite-size scaling theory based on the renormalization group approach. *Prog. Theor. Phys.*, Vol. 58, 1142-1150.

’t Hooft, G. & Veltman, M. (1972). Regularization and renormalization of gauge fields. *Nucl. Phys. B*, Vol. 44, 189-213.

Tang S. & Landau, D. P. (1987). Monte Carlo study of dynamic universality in two-dimensional Potts models. *Phys. Rev. B*, Vol. 36, 567-573.

Wansleben, S. & Landau, D. P. (1991). Monte Carlo investigation of critical dynamics in the three-dimensional Ising model. *Phys. Rev. B*, Vol. 43, 6006-6014.

Wegner, F. W. (1972). Corrections to scaling laws. *Phys. Rev. B*, Vol. 5, 4529-4536.

Weinberg, S. (1973). New approach to the renormalization group. *Phys. Rev. D*, Vol. 8, 3497-3509.

Wiseman S. & Domany, E. (1995). Lack of self-averaging in critical disordered systems. *Phys. Rev. B*, Vol. 52, 3469-3484.

Wiseman S. & Domany, E. (1998). Self-averaging, distribution of pseudocritical temperatures, and finite size scaling in critical disordered systems. *Phys. Rev. B*, Vol. 58, 2938-2951.

Wu, F. Y. (1982). The Potts model. *Rev. Mod. Phys.* , Vol. 54, 235-268.

Xiong, W.; Zhong, F.; Yuan, W. & Fan, S. (2010). Critical behavior of three-dimensional random-bond Ising model using finite-time scaling with extensive Monte Carlo renormalization-group method. *Phys. Rev. E*, Vol. 81, 051132.

Xiong, W.; Zhong, F. & Fan, S. (2010). Positive specific-heat critical exponent of the three-dimensional random-bond Potts model. submitted.

Yin, J. Q.; Zheng, B. & Trimper, S. (2004). Critical behavior of the two-dimensional random-bond Potts model: A short-time dynamic approach. *Phys. Rev. E*, Vol. 70, 056134.

Yin, J. Q.; Zheng, B. & Trimper, S. (2005). Dynamic Monte Carlo simulations of the three-dimensional random-bond Potts model. *Phys. Rev. E*, Vol. 72, 036122.

Yin, J. Q.; Zheng, B.; Prudnikov, V. V. & Trimper, S. (2006). Short-time dynamics and critical behavior of three-dimensional bond-diluted Potts model. *Eur. Phys. J. B*, Vol. 49, 195-203.

Zhang, J. X.; Fung, P. C. W. & Zeng, W. G. (1995). Dissipation function of the first-order phase transformation in solids via internal-friction measurements. *Phys. Rev. B*, Vol. 52, 268-277.

Zhang, J. B.; Wang, L.; Gu, D. W.; Ying, H. P. & Ji, D. R. (1999). Monte Carlo study of critical scaling and universality in non-equilibrium short-time dynamics. *Phys. Lett. A*, Vol. 262, 226-233.

Zhang, J. X.; Zhong, F. & Siu, G. G. (1996). The scanning-rate dependence of energy dissipation in first-order phase transition of solids. *Solid State Commun.* Vol. 97, 847-850.

Zheng, B. (1998). Monte Carlo simulations of short-time critical dynamics. *Int. J. Mod. Phys. B*, Vol. 12, 1419-1484.

Zhong, F. (2002). Monte Carlo renormalization group study of the dynamic scaling of hysteresis in the two-dimensional Ising model. *Phys. Rev. B*, Vol. 66, 060401(R)

Zhong, F. (2006). Probing criticality with linearly varying external fields: Renormalization group theory of nonequilibrium critical dynamics under driving. *Phys. Rev. E*, Vol. 73 047102

Zhong, F. & Chen, Q. Z. (2005). Theory of the dynamics of first-order phase transitions: Unstable fixed points, exponents, and dynamical scaling. *Phys. Rev. Lett.*, Vol. 95, 175701.

Zhong, F.; Zhang, J. X. & Siu, G. G. (1994). Dynamic scaling of hysteresis in a linearly driven system. *J. Phys.: Condens. Matter*, Vol. 6, 7785-7796.
Zhong, F.; Zhang, J. X. & Liu, X. (1995). Scaling of hysteresis in the Ising model and cell-dynamical systems in a linearly varying external field. *Phys. Rev. E*, Vol. 52, 1399-1402.
Zhong, F.; Dong, J. M. & Xing, D. Y. (1998). Scaling of hysteresis in pure and disordered Ising models: Comparison with experiments. *Phys. Rev. Lett.*, Vol. 80, 1118-1118.
Zhong, F. & Zhang, J. X. (1995). Scaling of thermal hysteresis with temperature scanning rate. *Phys. Rev. E*, Vol. 51, 2898-2901.
Zhong, F. & Zhang, J. X. (1995). Renormalization group theory of hysteersis. *Phys. Rev. Lett.*, Vol. 75, 2027-2030.
Zhong, F. & Zhang, J. X. (1997). Dynamic scaling of hysteresis in the 2D Ising model with impurities. *Acta Phys. Sin.*, Vol. 46, 791-795.
Zhong, F. & Xu, Z. F. (2005). Dynamic Monte Carlo renormalization group determination of critical exponents with linearly changing temperature. *Phys. Rev. B*, Vol. 71, 132402.
Zinn-Justin, J. (1996). *Quantum Field Theory and Critical Phenomena*, 3rd edn, Oxford, Clarendon.

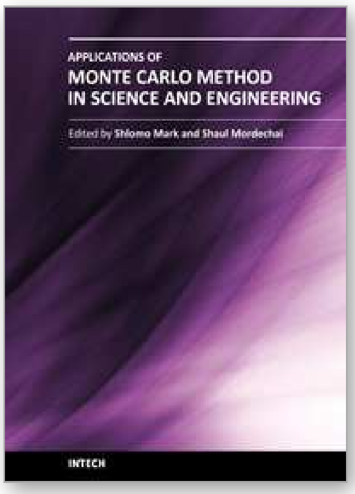

Applications of Monte Carlo Method in Science and Engineering
Edited by Prof. Shaul Mordechai

ISBN 978-953-307-691-1
Hard cover, 950 pages
Publisher InTech
Published online 28, February, 2011
Published in print edition February, 2011

In this book, Applications of Monte Carlo Method in Science and Engineering, we further expose the broad range of applications of Monte Carlo simulation in the fields of Quantum Physics, Statistical Physics, Reliability, Medical Physics, Polycrystalline Materials, Ising Model, Chemistry, Agriculture, Food Processing, X-ray Imaging, Electron Dynamics in Doped Semiconductors, Metallurgy, Remote Sensing and much more diverse topics. The book chapters included in this volume clearly reflect the current scientific importance of Monte Carlo techniques in various fields of research.

INTECH
open science | open minds

InTech Europe
University Campus STeP Ri
Slavka Krautzeka 83/A
51000 Rijeka, Croatia
Phone: +385 (51) 770 447
Fax: +385 (51) 686 166
www.intechopen.com

InTech China
Unit 405, Office Block, Hotel Equatorial Shanghai
No.65, Yan An Road (West), Shanghai, 200040, China
中国上海市延安西路65号上海国际贵都大饭店办公楼405单元
Phone: +86-21-62489820
Fax: +86-21-62489821